Replacing Parameters with Preferences: Federated Alignment of Heterogeneous Vision-Language Models

Shule Lu [*1,2] **Yujing Wang** [*1,2] **Hainan Zhang** [1,2] **Xiaoshan Yang** [3,4] **Hongwei Zheng** [5] **Yongxin Tong** [2]
Changsheng Xu [3,4] **Zhiming Zheng** [1,2]

Abstract

VLMs have broad potential in privacy-sensitive domains such as healthcare and finance, yet strict data-sharing constraints render centralized training infeasible. FL mitigates this issue by enabling decentralized training, but practical deployments face challenges due to client heterogeneity in computational resources, application requirements, and model architectures. We argue that while replacing data with model parameters characterizes the present of FL, replacing parameters with preferences represents a more scalable and privacy-preserving future. Motivated by this perspective, we propose MoR, a federated alignment framework based on GRPO with Mixture-of-Rewards for heterogeneous VLMs. MoR initializes a visual foundation model as a KL-regularized reference, while each client locally trains a reward model from local preference annotations, capturing specific evaluation signals without exposing raw data. To reconcile heterogeneous rewards, we introduce a routing-based fusion mechanism that adaptively aggregates client reward signals. Finally, the server performs GRPO with this mixed reward to optimize the base VLM. Experiments on three public VQA benchmarks demonstrate that MoR consistently outperforms federated alignment baselines in generalization, robustness, and cross-client adaptability. Our approach provides a scalable solution for privacy-preserving alignment of heterogeneous VLMs under federated settings.

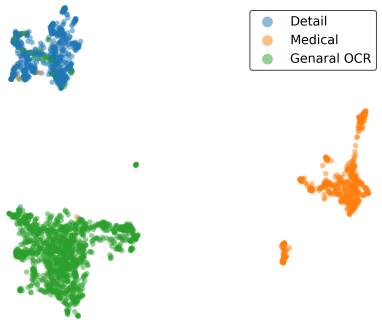

Figure 1. Visualization of multimodal data distributions across different task domains. The embeddings are extracted from the joint vision-language space and projected onto a 2D plane using UMAP (McInnes et al., 2018). Distinct clusters for Detail, Medical, and General OCR demonstrate significant domain shifts.

1. Introduction

Vision–language models (VLMs) have demonstrated remarkable capabilities across a wide range of applications (Tian et al., 2024; Bordes et al., 2024), including medical image analysis (Hartsock & Rasool, 2024) and decision support in finance (Nie et al., 2024). Many of these domains are privacy-sensitive, where strict regulations prohibit centralized data collection, especially for visual data (Rieke et al., 2020), limiting the practicality of centralized VLM training.

Federated learning (FL) (Konečnỳ et al., 2016; McMahan et al., 2017) has emerged as a promising solution by enabling decentralized model training without transferring raw data outside local domains. However, despite its success, current FL paradigms predominantly rely on replacing data sharing with parameter sharing. This design choice introduces several critical challenges in practice: (1) exchanged parameters can be exploited by adversarial clients to reconstruct data of other clients via gradient inversion attacks (Guo et al., 2025), (2) frequent parameter exchange incurs substantial communication and computational overhead, and (3) heterogeneous clients often differ in model architectures, computational budgets, and application objectives, making parameter-level aggregation brittle.

We argue that while replacing data with parameters char-

[1]Beijing Advanced Innovation Center for Future Blockchain and Privacy Computing [2]Institute of Artificial Intelligence, Beihang University, China [3]MAIS, Institute of Automation, Chinese Academy of Sciences, China [4]School of Artificial Intelligence, University of Chinese Academy of Sciences, China [5]Institute of Artificial Intelligence and Blockchain, Guangzhou University. Correspondence to: Hainan Zhang <zhanghainan@buaa.edu.cn>.

Preprint. February 3, 2026.

acterizes the present of FL in LLMs, replacing parameters with preferences represents a more scalable and privacy-preserving future. Preferences capture high-level user intent, are privacy-preserving, and align with downstream goals, making them ideal for federated learning where clients share reward signals instead of raw data or model parameters. Several studies have explored federated preference alignment by extending centralized frameworks to decentralized settings. PluralLLM (Srewa et al., 2025a) adapts Group Policy Optimization (GPO) (Zhao et al., 2023b) to train collaborative preference predictors without sharing raw data, but its reliance on shared predictor structures leads to high computational and communication overhead and limited flexibility under heterogeneous reward models. Subsequent work (Srewa et al., 2025b) improves preference selection but still assumes homogeneous reward structures, making it sensitive to client-side preference heterogeneity.

We observe that multimodal contents vary substantially among clients in federated settings. For example, one client may favor fine-grained visual details, while another prioritizes domain-specific accuracy such as medical correctness, leading to distinct preference distributions, as illustrated in Figure 1. In practice, such diversity often leads to heterogeneous reward model structures across federated clients. Consequently, a single, monolithic reward model is therefore insufficient to capture such heterogeneous preference distributions accurately, and may even suffer from conflicting supervision signals when trained on aggregated data. Inspired by Mixture-of-Experts (MoE) (Jacobs et al., 1991; Shazeer et al., 2017; Lepikhin et al., 2020), which decomposes complex and diverse preference patterns into specialized experts and dynamically selects the most relevant one to handle heterogeneous signals, we design a routing network to select the appropriate client reward model for each input, enabling flexible preference alignment.

In this paper, we propose MoR, a novel VLM reinforcement alignment paradigm based on Mixture-of-Rewards, designed to accommodate heterogeneous client preferences and structurally diverse reward models, while preserving privacy and ensuring computational and communication efficiency. Specifically, we first train client-specific reward models on local data at each client, allowing each model to adapt to the preference style inherent in its local data. These reward models are then uploaded to a central server. Next, inspired by MoE, we train a lightweight routing network using FL to integrate preference signals of different styles and resolve potential preference conflicts, while maintaining privacy preservation. The trained routing network is uploaded to the central server and, together with the reward models, forms a mixture of reward models that selects the appropriate reward during inference. In the final stage, clients transmit only low-dimensional embeddings of non-preference input data to the central server, safeguarding sensitive raw information. Centralized preference alignment of the base VLM is then performed using synthesized reward signals produced by the MoR, while the routing network is continuously updated online to adapt to output distribution shifts induced by updates of the base VLM.

Experimental results on three VQA datasets demonstrate that MoR achieves more pronounced advantages over existing reward modeling methods and FL approaches in terms of generalization, robustness, and cross-client adaptability. The innovations of this paper are as follows:

- We argue that federated preference alignment is a more suitable paradigm for federated VLMs, especially under client heterogeneity, as it better accommodates diverse model architectures and application objectives.
- We propose MoR, a mixture-of-rewards framework that uses routing-based reward composition to efficiently integrate heterogeneous client reward models in federated settings.
- Extensive experiments conducted on three datasets validate that MoR consistently outperforms existing mixture reward model training methods and FL approaches, demonstrating its effectiveness and robustness.

2. Related Works

2.1. LLM Routing and Model Selection

Routing and model selection have been widely explored in large language model systems as effective mechanisms for improving efficiency, scalability, and robustness. Early studies primarily focus on inference-time routing, where routers dynamically select experts or models of different capacities to balance computational cost and performance. A variety of mechanisms have been proposed to steer these routing decisions (Lu et al., 2024; Ding et al., 2024; Ong et al., 2025). And more recent work (Frick et al., 2025) further improves the scalability of inference routing, and extends inference-time routing to multimodal large models (Tang et al., 2025). Recently, routing mechanisms have been introduced into the reward modeling stage of RLHF. In this line of work, reward model selection is often formulated as a multi-armed bandit problem, where different reward models correspond to distinct arms. For instance, algorithms like LinUCB (Li, 2025) and Bayesian Thompson Sampling (Wu & Lu, 2025) have been employed to select optimal reward models or guide routing based on training signals. However, existing reward routing approaches are typically designed under centralized assumptions and are restricted to text-only models, without considering federated learning scenarios with heterogeneous reward models distributed across different clients, nor extending routing-based reward selection to multimodal alignment settings.

2.2. Decentralized and Federated Preference Alignment

Most existing preference alignment methods are developed under centralized assumptions, where human feedback and reward models are collected and optimized within a single training pipeline (Zhao et al., 2023b; Ramesh et al., 2024; Chakraborty et al., 2024). However, such centralized settings are often impractical in scenarios involving privacy-sensitive data or distributed data ownership. To address these concerns, FL is introduced into preference alignment, enabling collaborative model training without sharing raw preference data. Recent work (Srewa et al., 2025a) extends GPO frameworks to federated settings, allowing multiple clients or groups to jointly learn preference predictors while preserving data locality. Subsequent study (Srewa et al., 2025b) further introduces dynamic preference selection strategies and extends these frameworks to reinforcement learning-based training. Another approach (Wu et al., 2024) mitigates preference heterogeneity by clustering or aggregating client-side preference models. However, existing decentralized preference alignment methods often incur high computational and communication costs and remain highly sensitive to heterogeneous preference distributions across clients. Moreover, these methods typically focus on static preference aggregation or selector learning, without jointly optimizing reinforcement learning policies under dynamically selected or routed reward signals. This disconnection limits their ability to adapt effectively to complex, varying client preferences in scalable real-world applications.

3. Task Definition

In this work, we address a preference alignment problem under a federated and heterogeneous setting. Let $\mathcal{C} = \{1, \ldots, K\}$ denote a set of clients. Let f_θ denote a VLM parameterized by θ, which maps a multimodal input $x \in \mathcal{X}$ to an output $y \in \mathcal{Y}$, $y = f_\theta(x)$. Each client $k \in \mathcal{C}$ owns a private multimodal dataset $\mathcal{D}_k$, consisting of visual and textual modalities. The data distributions across clients are Non-IID, with heterogeneity arising from variations in visual content, linguistic expressions, and preference annotations across clients, $\mathcal{D}_k \sim \mathcal{P}_k$, $\mathcal{P}_k \neq \mathcal{P}_{k'}$,$k \neq k'$, where $\mathcal{P}_k$ denotes the local data distribution of the k-th client, which encompasses the joint distribution of multimodal inputs and user preference labels. Specifically, we focus on vision–language tasks and take Visual Question Answering (VQA) as a representative example. Each local dataset $\mathcal{D}_k$ consists of non-preference data $\mathcal{D}_k^{np} = x_i^k$ and preference data $\mathcal{D}_k^{pref} = (x_i^k, y_i^{k,+}, y_i^{k,-})$, where $y_i^{k,+} \succ y_i^{k,-}$ reflects that $y_i^{k,+}$ and $y_i^{k,-}$ are the preferred and rejected answers. Due to privacy and data ownership constraints, raw preference data cannot be shared or centrally aggregated.

Each client possesses an implicit preference function R_k: $\mathcal{X} \times \mathcal{Y} \longrightarrow \mathbb{R}$, which assigns higher scores to outputs better aligned with its local preference style. For our VQA task, better alignment represents higher accuracy. The goal of preference alignment is to optimize the VLM such that its outputs maximize the expected reward across clients:

$$\theta^* = \arg\max_\theta \sum_{k=1}^{K} \mathbb{E}_{x \sim \mathcal{P}_k} \left[R_k\big(x, f_\theta(x)\big) \right].$$

Due to FL privacy constraints, raw data and preference annotations never leave local clients.

4. Methods

4.1. Framework Overview

In MoR framework, as shown in Figure 2, each client first trains a local reward model using its private preference data, allowing the model to capture client-specific evaluation criteria without exposing raw data. Upon completion, all client-side reward models R_k are uploaded to a central server. Each client then retrieves the full set of reward models $\{R_k\}$ from the server. Next, a lightweight router g_ϕ is trained via FL to learn how to dynamically select and combine reward signals from different clients. After FL, the routing network g_ϕ is also uploaded to the central server. Together, the routing network and the collection of client-specific reward models constitute a Mixture-of-Rewards. Finally, during preference alignment, each client computes embeddings of the input modality for non-preference data locally and transmits only these embeddings to the central server. The server performs preference alignment using reward signals produced by the mixture-of-rewards model, while the routing network is continuously updated in an online manner to adapt to output distribution shifts induced by updates to the VLM. Throughout this process, we assume that the central server is honest and non-malicious.

4.2. Reward models Initialization

Each client independently initializes and trains a local reward model based on its private multimodal preference dataset $\mathcal{D}_k^{\text{pref}}$, as shown in Figure 2(A). The reward model R_k maps a multimodal input–output pair (x, y) to a scalar score $R_k(x, y)$, reflecting the alignment between the candidate output and the client-specific preferences. For training, each preference tuple $(x_i^k, y_i^{k,+}, y_i^{k,-}) \in \mathcal{D}_k^{\text{pref}}$ indicates that $y_i^{k,+}$ is preferred over $y_i^{k,-}$. Following standard reward modeling practice, we adopt a pairwise preference learning objective grounded in the Bradley–Terry model (Bradley & Terry, 1952), which can be expressed as:

$$\mathcal{L}_{\text{RM}}^{(k)} = -\mathbb{E}_{\mathcal{D}_k^{pref}} \left[\log \sigma \Delta R_k(x_i^k, y_i^{k,+}, y_i^{k,-}) \right],$$

where $\sigma(\cdot)$ denotes the logistic sigmoid function.

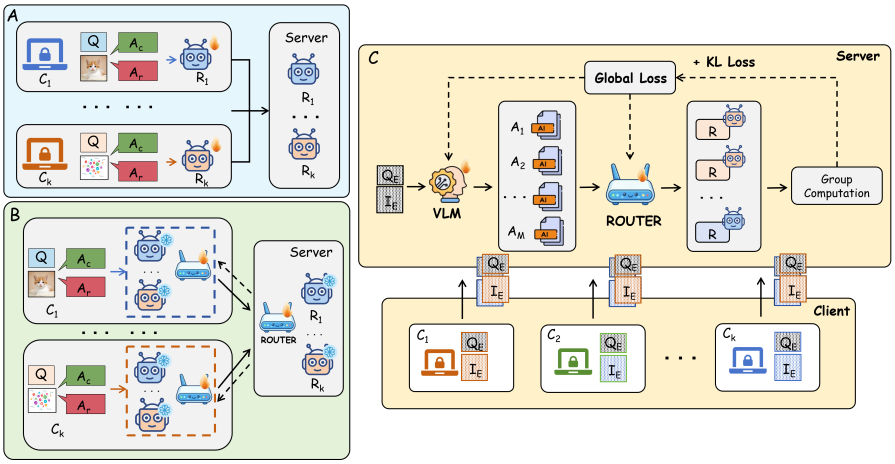

Figure 2. Overview of our proposed federated framework architecture. The framework is composed of three interconnected stages: (A) Decentralized Reward Model Training: Individual clients independently train local reward models (RMs) on their private, domain-specific datasets. (B) Federated Router Training: A global routing mechanism is collaboratively trained across clients to learn how to dispatch inputs to the most capable local RM. (C) GRPO Policy Alignment: The final multimodal policy is optimized using Group Relative Policy Optimization (GRPO), guided by the high-quality reward signals selected by the trained router.

4.3. Routing Network Federated Learning

To accommodate both heterogeneous client preferences and structurally diverse client-specific reward models in federated settings, we introduce a lightweight router g_ϕ parameterized by ϕ that operates on top of frozen local reward models. Moreover, by federating only the router g_ϕ rather than the reward model, our approach substantially reduces communication overhead, as the router contains fewer parameters than typical multimodal reward models. This design enables scalable and privacy-preserving alignment under heterogeneous client data and model configurations.

At the beginning of training, each client downloads the complete set of client-specific reward models from the central server, as shown in Figure 2(B). The reward models are kept frozen during routing network training and are used solely to provide preference supervision. For each communication round $t \geq 0$, the central server distributes the latest global routing network parameters to all participating clients. Each client then performs synchronized local training of the routing network on its private preference dataset. Given a preference tuple (x, y^+, y^-), all reward models independently assign scores to the preferred and rejected responses. The routing network takes the input–response pair (x, y) as input and outputs a set of weights over the reward models, indicating the relative importance of each reward signal. Formally, let $\{R_k\}_{k=1}^K$ denote the set of client-specific reward models, and let

$$\boldsymbol{\alpha}(x, y; \phi) = \mathrm{softmax}(g_\phi(x, y))$$

be the routing weights produced by the routing network g_ϕ, where $\alpha_k(x, y)$ represents the weight assigned to reward model R_k. The mixed reward score for an input–response pair (x, y) is computed as:

$$R_{\mathrm{mix}}(x, y; \phi) = \sum_{k=1}^{K} \alpha_k(x, y; \phi)\, R_k(x, y).$$

Accordingly, the reward margin is $\Delta R_{\mathrm{mix}}(x, y^+, y^-; \phi_t^k) = R_{\mathrm{mix}}(x, y^+; \phi_t^k) - R_{\mathrm{mix}}(x, y^-; \phi_t^k)$. Each client k updates its local routing parameters ϕ_t^k by minimizing the negative log-likelihood of observed preferences:

$$\mathcal{L}_{\mathrm{r}} = -\mathbb{E}_{\mathcal{D}_k^{\mathrm{pref}}} \left[\log \sigma \Delta R_{\mathrm{mix}}(x, y^+, y^-; \phi_t^k) \right].$$

After local training, each client uploads its updated routing parameters ϕ_t^k to the server. The server then aggregates the client updates to obtain the next global routing model parameters: $\phi_{t+1} = \sum_{k=1}^K \frac{|\mathcal{D}_k^{\mathrm{pref}}|}{\sum_{k'=1}^K |\mathcal{D}_{k'}^{\mathrm{pref}}|}\, \phi_t^k$, following FedAvg (McMahan et al., 2017) scheme.

4.4. GRPO with Routing Network Online updating

We optimize the policy model using Group Relative Policy Optimization (GRPO, Shao et al., 2024), which extends pairwise preference-based reinforcement learning by leveraging relative comparisons within groups of candidate responses. At each iteration, we define π_t as the policy at iteration t, with $\pi_t|_{t=0} = \pi_0$. Given a mini-batch of multimodal contexts $\{x_i\}_{i=1}^B \subset \mathcal{X}$. For each input x_i, the policy samples a group of M candidate responses $\{y_{i,j}\}_{j=1}^M$ from the distribution $\pi_t(\cdot \mid x_i)$.

For each sampled response $y_{i,j}$, we construct an input-response pair $(x_i, y_{i,j})$ and feed it into the routing network alongside the set of client-specific reward models. The routing network produces a weight vector conditioned on both

the multimodal context and the generated response:

$$\boldsymbol{\alpha}_{i,j} = \mathrm{softmax}(g_\phi(x_i, y_{i,j}))\,,$$

where $\alpha_{i,j}^{(k)}$ denotes the importance weight assigned to reward model R_k. The final routed reward for response $y_{i,j}$ is computed as a weighted linear combination of the outputs from the constituent reward models:

$$\tilde{R}_{i,j} = \sum_{k=1}^{K} \alpha_{i,j}^{(k)}\, R_k(x_i, y_{i,j}).$$

However, for efficient online exploration, we employ hard-selection during this phase by sampling a single reward model. Subsequently, the policy is optimized using an advantage function derived from these routed rewards. Let $\pi_{\theta_{\text{old}}}$ denote the policy state prior to the current update. The GRPO objective function is defined as follows:

$$\mathcal{J}_{\text{GRPO}}(\theta) = \mathbb{E}_{\substack{x\sim\mathcal{X} \\ \{y_i\}\sim\pi_{\theta_{\text{old}}}}} \left[\mathcal{L}_{\text{clip}}(\theta, \hat{A}) - \beta\mathbb{D}_{\text{KL}}(\pi_\theta\|\pi_{\text{ref}})\right],$$

where $\mathcal{L}_{\text{clip}}$ denotes the token-level clipped surrogate loss, $\hat{A}$ represents the group-relative advantage from the routed rewards $\tilde{R}_{i,j}$, and β controls the KL divergence penalty.

The above formulation implicitly assumes that the routing function g_ϕ remains fixed during policy optimization. However, in practice, the routing network is trained offline using static preference datasets with fixed answer candidates, whereas during GRPO training, the policy π_θ continually evolves. As a result, the distribution of generated responses shifts over time, leading to a mismatch between the router's training distribution and the on-policy data encountered. To address this issue, we update the routing network online during GRPO training. Specifically, we model reward routing as a contextual bandit problem (Li, 2025; Wu & Lu, 2025), where the context is given by the embedding of the input–response pair (x, y), and each arm corresponds to selecting a client-specific reward model.

We adopt Neural Thompson Sampling (Zhang et al., 2021) to update the routing network online, which maintains a posterior over routing parameters and balances exploration and exploitation under non-stationary response distributions. During GRPO training, at each iteration t, the policy π_θ generates a response $y_t \sim \pi_\theta(\cdot \mid x_t)$ for a given input x_t.The routing network observes the input–response pair (x_t, y_t) and selects one reward model from the set $\{R_k\}_{k=1}^K$ to evaluate the response. We formulate this process as a contextual bandit problem, where the context is given by an embedding $c_t = \mathrm{Enc}(x_t, y_t)$, and each arm corresponds to selecting a client-specific reward model R_k. The routing network g_ϕ produces a vector of logits, whose k-th component $\hat{r}_k(c_t;\phi)$ estimates the expected reward obtained by choosing R_k for the current input–response pair. To encourage exploration, Neural Thompson Sampling constructs a Gaussian posterior over the predicted reward for each arm:

$$\tilde{r}_{t,k} \sim \mathcal{N}\big(\hat{r}_k(c_t;\phi_{t-1}),\ \nu^2\sigma_{t,k}^2\big),$$

where $\sigma_{t,k}^2$ represents the exploration variance for arm k at time t, which can be computed as

$$\sigma_{t,k}^2 = \lambda\, \nabla_\phi \hat{r}_k(c_t;\phi_{t-1})^\top \mathbf{U}_{t-1}^{-1} \nabla_\phi \hat{r}_k(c_t;\phi_{t-1}),$$

where λ is a regularization coefficient that controls the prior uncertainty and scales the exploration variance in Neural Thompson Sampling, and $\mathbf{U}_t$ is an empirical covariance matrix that accumulates gradient information over time, and ν controls the exploration scale. The routing decision is made by selecting the arm with the highest sampled reward:

$$k_t = \arg\max_k \tilde{r}_{t,k}.$$

After selecting reward model R_{k_t}, the router observes a scalar bandit feedback derived from the change in the global GRPO objective:

$$\Delta\mathcal{J}_t = \mathcal{J}_{\text{GRPO}}^{t} - \mathcal{J}_{\text{GRPO}}^{t-1},$$

then the feedback signal is defined as a binary reward

$$r_t = \begin{cases} 0, & \text{if } \Delta\mathcal{J}_t > 0 \\ 1, & \text{if } \Delta\mathcal{J}_t \le 0 \end{cases},$$

indicating whether the selected reward model leads to an improvement in policy optimization. The routing parameters are then updated by minimizing an ℓ_2-regularized squared loss:

$$\mathcal{L}_{\text{online}}(\phi) = \frac{1}{2}\big(\hat{r}_{k_t}(c_t;\phi) - r_t\big)^2 + \frac{\lambda}{2}\|\phi - \phi_0\|_2^2,$$

where ϕ_0 denotes the router initialization obtained from offline training on static preference data. Simultaneously, the covariance matrix is updated as

$$\mathbf{U}_t = \mathbf{U}_{t-1} + \nabla_\phi \hat{r}_{k_t}(c_t;\phi_t) \nabla_\phi \hat{r}_{k_t}(c_t;\phi_t)^\top.$$

5. Experiments

5.1. Experimental Settings

5.1.1. Dataset

We construct a heterogeneous vision-language preference dataset by combining POVID (Zhou et al., 2024) and VLFeedback (Li et al., 2023b), two complementary sources with distinct annotation paradigms. Notably, the VLFeedback dataset utilizes a scoring paradigm where each response is scored across the three dimensions of helpfulness, visual faithfulness, and ethical considerations rather than through explicit pairwise labels. By comparing responses

under the same image–query input, we convert these score-based annotations into pairwise preferences, enabling preference learning without direct access to raw training data.

To model realistic client heterogeneity in decentralized settings, we partition the data into three domain-specific subsets: (i) **Detail Description**, mainly from POVID and detail-oriented subsets of LLaVA (Liu et al., 2023) and SVIT (Zhao et al., 2023a) within VLFeedback; (ii) **Medical Vision-Language Understanding**, constructed from LLaVAMed (Li et al., 2023a) and PMC-VQA (Zhang et al., 2023a) within VLFeedback; and (iii) **OCR-like Visual Reasoning**, derived from the text-rich LLaVAR (Zhang et al., 2023b) subset within VLFeedback.

5.1.2. Baselines

We compare our method against a diverse set of baselines that represent different paradigms for vision-language model alignment under decentralized or preference-based settings:

Single RM: Each client trains and uses its own domain-specific reward model locally during GRPO, without any cross-client interaction.

Random selection: During training, a reward model is randomly selected from different clients to evaluate each response, ignoring client–domain alignment.

Avg RM: Rewards produced by all client-specific reward models are averaged to form a global feedback signal.

FedAvg: (McMahan et al., 2017) Client-specific reward models are periodically aggregated by parameter averaging following the standard FedAvg protocol.

Pluralistic: (Srewa et al., 2025b) Client preferences are aggregated under a homogeneous reward model assumption, producing a single global alignment signal for policy optimization without client-aware routing.

Oracle RM: A single reward model is trained on the union of all domain preference data and used uniformly during GRPO training.

5.1.3. Metrics

We evaluate all models using an LLM-as-a-Judge protocol. For each image–instruction input, the judge compares candidate responses along three complementary dimensions: Helpfulness, Visual Faithfulness, and Ethical Considerations. We report pairwise preference win-rates, average judge scores across the three evaluation dimensions, and Visual Faithfulness scores. Additionally, to ensure robustness against stochastic decoding, we adopt a best-of-3 sampling strategy for all evaluated policies under identical decoding settings. Domain-wise win-rates are reported for detailed descriptions, medical, and OCR-like subsets. The detailed prompt template is provided in Appendix B.

5.1.4. Implementation Details

All experiments use `Qwen2.5-VL-7B-Instruct` (Qwen-Team, 2025) as a fixed policy model to isolate the effect of reward modeling. We evaluate two paradigms: a homogeneous setting, where all clients share `Qwen2.5-VL-3B-Instruct` (Qwen-Team, 2025) as the uniform reward model architecture, and a heterogeneous setting, where clients utilize a diverse set of reward models, including `Qwen2-VL-2B-Instruct` (Wang et al., 2024), `llava-onevision-0.5b` (Li et al., 2024), and `Qwen2.5-VL-3B-Instruct`.

In our experimental setup, we consider a federated scenario with three clients, each holding a domain-specific dataset. Reward models are primarily trained using contrastive learning. During the reinforcement learning stage, we adopt a modified EasyRL framework (Zheng et al., 2025), setting the learning rate to 1e-6. For the router update phase, our router consists of four Transformer layers and a linear classification head, and only the linear layer is updated. Given that we utilize a fixed vision tower for input encoding during training, the distribution of visual features remains highly stable. Consequently, we set a reduced learning rate 1e-7, as a larger step size could lead the router to overfit to transient fluctuations in the text policy. Our experiments are conducted on a server equipped with 4× RTX A6000 PRO GPUs, each with 96GB memory. More details can be found in Appendix A.

5.2. Main Results

Table 1 presents the comprehensive experimental results of our method and various baselines across three domain datasets. The table is organized into two sections to compare performance under different model compositions.

The upper section details the performance under heterogeneous reward model architectures. Our primary findings in this setting are as follows: (1) A critical challenge in heterogeneous federated learning is the presence of underperforming clients, such as RM1 (`LLaVA-0.5B`), which scores significantly lower across tasks due to its smaller architecture. Naive aggregation methods like Avg RM suffer severely from this "bucket effect." This is most evident in the Detail domain, where the inclusion of the weak RM1 (Avg Score: 3.44) drags the collective Avg RM score down to 4.97. In stark contrast, our method (Ours (Hete.)) achieves a superior score of 7.73. This demonstrates the router's capability to effectively identify and filter out noisy signals from weaker models, thereby preventing the performance degradation inherent in simple averaging. (2) Our approach not only avoids the pitfalls of weak models but also effectively synergizes the strengths of capable ones. In all three

Table 1. Main results under Heterogeneous and Homogeneous reward models. The top section reports results for heterogeneous RMs (RM0-RM2), where RM0 to RM2 denote heterogeneous single-client reward models with different architectures: RM0 uses `Qwen2-VL-2B-Instruct`, RM1 uses `llava-onevision-0.5b`, and RM2 uses `Qwen2.5-VL-3B-Instruct`. And the bottom section reports results for homogeneous RMs (all using `Qwen2.5-VL-3B-Instruct`). Win Rate reports the pairwise preference win-rate against rejected responses. Faithfulness refers to the Visual Faithfulness score. More results details are in Appendix C.

Method	Medical			OCR-like			Detail		
	Avg Score	Win Rate	Faithfulness	Avg Score	Win Rate	Faithfulness	Avg Score	Win Rate	Faithfulness
Setting 1: Heterogeneous Reward Models									
RM0 (`Q2-VL-2B`)	5.55	65.59	4.66	7.38	70.01	6.38	7.11	73.57	5.98
RM1 (`LLaVA-0.5B`)	3.13	46.51	2.43	6.51	63.85	6.59	3.44	33.26	2.46
RM2 (`Q2.5-VL-3B`)	7.52	88.25	6.83	8.21	65.20	7.58	7.01	80.20	5.73
Random Selection	6.28	74.96	5.44	7.52	74.03	6.37	7.60	77.39	6.57
Avg RM	7.40	86.52	6.66	**8.76**	**90.09**	**8.41**	4.97	60.00	3.26
Ours (Hete.)	**8.25**	**92.50**	**7.73**	8.73	87.23	8.27	**7.73**	**80.88**	**6.80**
Setting 2: Homogeneous Reward Models									
RM0	6.85	83.65	6.28	8.46	86.19	8.24	6.12	61.09	5.59
RM1	8.00	91.82	7.58	8.69	89.08	8.21	8.00	85.32	7.21
RM2	7.52	88.25	6.83	8.21	65.20	7.58	7.01	80.20	5.73
FedAvg	8.25	94.04	7.86	9.05	**92.54**	**8.90**	8.08	83.70	7.34
Random Selection	7.59	88.93	6.93	8.68	88.79	8.22	7.93	83.06	7.08
Pluralistic	8.32	92.50	7.93	8.77	89.21	8.37	**8.25**	**90.60**	**7.53**
Oracle RM	6.94	87.22	6.18	8.62	85.32	8.28	7.40	74.89	6.23
Ours (Homo.)	**8.58**	**94.55**	**8.33**	**9.06**	91.54	8.86	8.15	89.72	7.40

tested domains, our method yields a composite model that is stronger than any single constituent expert. Specifically, in the Medical domain, our method achieves an Avg Score of 8.25, surpassing the best individual model, RM2 (7.52). Similarly, in the Detail domain, our score of 7.73 exceeds the best individual performer, RM0 (7.11). This indicates that the router successfully learns to dispatch samples dynamically to the most suitable expert for the specific input. (3) While Avg RM shows peak performance in the OCR-like domain (8.76 Avg Score), it exhibits extreme instability, collapsing in the Detail domain. Individual models also show significant domain-specific fluctuations (e.g., RM2 is strong in Medical but less reliable in Detail faithfulness). Conversely, our method maintains consistent, top-tier competitiveness across all three domains (Medical: 8.25, OCR-like: 8.73, Detail: 7.73). It acts as a robust stabilizer in heterogeneous environments where model capabilities are unevenly distributed across different tasks.

To further isolate the effect of model heterogeneity, the lower section of Table 1 presents results in a homogeneous architecture setting, where all clients adopt the same model structure while keeping the training protocol unchanged. We have the following key findings: (1) Our method (Ours(Homo.)) consistently achieves the highest Average Score and Visual Faithfulness across all three domains, significantly surpassing both the strongest individual models and the FedAvg baseline, as observed in the Medical domain. This indicates that even with identical model architectures, our routing mechanism effectively selects the most precise reward signals to yield higher-quality evaluations. (2) While aggregation methods like FedAvg and Pluralistic exhibit competitive performance in Win Rate, occasionally achieving marginally higher results in specific domains, our method consistently outperforms them in both Average Score and Faithfulness. This suggests that while baseline methods frequently align with general preferences, our approach captures finer-grained nuances, resulting in significantly higher absolute scores and reduced hallucination. (3) Individual reward models continue to demonstrate domain-specific weaknesses, exemplified by RM2's significant drop in Faithfulness within the Detail domain (5.73). In contrast, our approach mitigates these performance dips, maintaining high Faithfulness (> 8.1) and consistent Win Rates across all categories. This demonstrates that our method successfully functions as a "generalist expert," leveraging collective strengths more effectively than static averaging strategies.

5.3. Ablation Study

To isolate the impact of the online router update mechanism during the reinforcement learning phase, we compare both the Average Score (AS.) and Win Rate (WR.) results in Table 2 with those reported for the full method in Table 1.

Comparing the results in Table 2 reveals that disabling online updates yields performance broadly comparable to, yet generally inferior to, the full online approach. In the homogeneous setting, this gap is narrow; for instance, the Medical Win Rate drops only marginally from 94.55% (Online) to 93.87% (Frozen). We attribute this relative stability

to the multimodal nature of the task: since the vision tower remains frozen throughout training, it provides a highly stationary distribution of visual features that serves as a critical signal for domain routing. Consequently, while textual distributions shift alongside policy evolution during RL, the resulting destabilizing effect on routing decisions is notably less severe in this multimodal setting compared to purely textual domains.

Table 2. Ablation study on online router updating in federated reward modeling, Frozen (Homo.) and Frozen (Hete.) refer to the disabling of online router updates in homogeneous and heterogeneous scenarios. We report average judge score (AS.) and pairwise preference win-rates against the rejected responses (WR.).

Method	Medical		OCR-like		Detail	
	AS.	WR.	AS.	WR.	AS.	WR.
Frozen (Hete.)	7.81	91.14	8.08	80.46	7.87	82.55
Online (Hete.)	8.25	92.50	8.73	87.23	7.73	80.88
Frozen (Homo.)	8.52	93.87	9.12	92.74	8.04	88.54
Online (Homo.)	8.58	94.55	9.06	91.54	8.15	89.72

Table 3. Analysis on batch level or query level. We report the average judge score and win-rate performance under Homogeneous reward model settings.

Method	Medical		OCR-like		Detail	
	AS.	WR.	AS.	WR.	AS.	WR.
batch	7.64	86.03	8.61	88.92	8.39	91.02
query	8.58	94.55	9.06	91.54	8.15	89.72

5.4. Computational Efficiency Analysis

We additionally report the training time overhead under identical training settings, as shown in the Figure 3. Our method maintains an $O(1)$ computational complexity during training, whereas the Avg RM baseline incurs an $O(N)$ complexity due to aggregating rewards from multiple models. As a result, our approach is more training-efficient. Compared to the single-RM setting, the additional overhead mainly comes from encoding inputs and performing inference with the routing network. However, since the router is lightweight, this overhead remains modest and does not significantly increase the overall training cost.

In contrast, parametric federated learning approaches require each client to maintain and optimize an independent policy model, followed by periodic parameter aggregation via FedAvg. In such settings, both the training and communication costs scale linearly with the number of clients, i.e., $O(K \cdot |\theta|)$, where K denotes the number of clients and $|\theta|$ the policy size. Our method avoids client-wise policy training and aggregation by decoupling client heterogeneity from policy parameterization. Consequently, the overall computational and communication complexity remains constant with respect to the number of clients, making our approach more scalable and efficient, particularly for large-scale multimodal models.

To optimize efficiency, we transition from per-query routing to a batch-level strategy, determining the optimal RM via majority voting on simultaneous selections for an entire input batch. Table 3 compares these strategies under homogeneous settings. As illustrated in Figure 3, while batch-level routing reduces computation time, it generally yields lower performance compared to the fine-grained query-level approach, most notably in the Medical domain. This highlights a requisite trade-off between computational efficiency and routing precision.

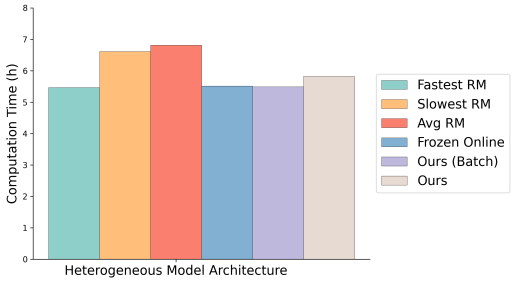

Figure 3. Computation Efficiency Analysis. We compare one epoch training time (in hours) of our method against individual reward models (RMs) and the ensemble baseline (Avg RM) in the heterogeneous setting.

6. Conclusion

In this paper, we propose MoR, a mixture-of-rewards reinforcement alignment paradigm for vision–language models in FL. By shifting the focus from parameter sharing to preference composition, MoR effectively addresses privacy concerns, communication overhead, and client heterogeneity that commonly arise in federated VLM alignment. Specifically, we enable clients to train structurally diverse reward models locally, while a lightweight routing network is collaboratively optimized via FL to dynamically select and integrate appropriate reward signals. This design allows MoR to capture heterogeneous preference styles and achieve efficient and privacy-preserving preference alignment. Extensive experiments on three VQA benchmarks demonstrate that MoR consistently outperforms existing reward modeling methods and FL approaches. Future work may explore extending MoR to more dynamic federated environments, particularly scenarios where the number of participating clients changes over time. A promising direction is to design adaptive routing and reward integration mechanisms that can naturally incorporate newly joined clients without retraining the entire mixture, while maintaining stability and alignment performance.

Impact Statement

This work addresses a critical barrier to deploying powerful Visual Language Models (VLMs) in high-stakes, privacy-sensitive domains such as healthcare and finance. By proposing a framework that shifts the federated learning paradigm from sharing model parameters to sharing localized preferences (rewards), we offer a viable path to unlock vast amounts of valuable data currently trapped in regulatory silos. This has the potential to significantly accelerate AI-driven advancements in areas like medical diagnosis and financial fraud detection, while respecting data sovereignty. Furthermore, by explicitly addressing client heterogeneity, our approach helps democratize access to advanced AI training, allowing institutions with varying computational resources to contribute to and benefit from foundational models.

Acknowledgement

This work was funded by the National Natural Science Foundation of China (NSFC) under Grants No.U25B2070 and No. 62406013, the Beijing Advanced Innovation Center Funds for Future Blockchain and Privacy Computing(GJJ-24-034), and the Fundamental Research Funds for the Central Universities.

References

Bordes, F., Pang, R. Y., Ajay, A., Li, A. C., Bardes, A., Petryk, S., Mañas, O., Lin, Z., Mahmoud, A., Jayaraman, B., et al. An introduction to vision-language modeling. *arXiv preprint arXiv:2405.17247*, 2024.

Bradley, R. A. and Terry, M. E. Rank analysis of incomplete block designs: I. the method of paired comparisons. *Biometrika*, 39(3/4), 1952.

Chakraborty, S., Qiu, J., Yuan, H., Koppel, A., Manocha, D., Huang, F., Bedi, A. S., and Wang, M. Maxmin-rlhf: alignment with diverse human preferences. In *Proceedings of the 41st International Conference on Machine Learning*, pp. 6116–6135, 2024.

Ding, D., Mallick, A., Wang, C., Sim, R., Mukherjee, S., Rühle, V., Lakshmanan, L. V., and Awadallah, A. H. Hybrid llm: Cost-efficient and quality-aware query routing. *CoRR*, 2024.

Frick, E., Chen, C., Tennyson, J., Li, T., Chiang, W.-L., Angelopoulos, A. N., and Stoica, I. Prompt-to-leaderboard. *arXiv preprint arXiv:2502.14855*, 2025.

Guo, P., Wang, R., Zeng, S., Zhu, J., Jiang, H., Wang, Y., Zhou, Y., Wang, F., Xiong, H., and Qu, L. Exploring the vulnerabilities of federated learning: A deep dive into gradient inversion attacks. *IEEE Transactions on Pattern Analysis and Machine Intelligence*, pp. 1–17, 2025. doi: 10.1109/TPAMI.2025.3646639.

Hartsock, I. and Rasool, G. Vision-language models for medical report generation and visual question answering: A review. *Frontiers in artificial intelligence*, 7:1430984, 2024.

Jacobs, R. A., Jordan, M. I., Nowlan, S. J., and Hinton, G. E. Adaptive mixtures of local experts. *Neural computation*, 3(1):79–87, 1991.

Konečnỳ, J., McMahan, H. B., Yu, F. X., Richtárik, P., Suresh, A. T., and Bacon, D. Federated learning: Strategies for improving communication efficiency. *arXiv preprint arXiv:1610.05492*, 2016.

Lepikhin, D., Lee, H., Xu, Y., Chen, D., Firat, O., Huang, Y., Krikun, M., Shazeer, N., and Chen, Z. Gshard: Scaling giant models with conditional computation and automatic sharding. *arXiv preprint arXiv:2006.16668*, 2020.

Li, B., Zhang, Y., Guo, D., Zhang, R., Li, F., Zhang, H., Zhang, K., Li, Y., Liu, Z., and Li, C. Llava-onevision: Easy visual task transfer, 2024. URL https://arxiv.org/abs/2408.03326.

Li, C., Wong, C., Zhang, S., Usuyama, N., Liu, H., Yang, J., Naumann, T., Poon, H., and Gao, J. Llava-med: Training a large language-and-vision assistant for biomedicine in one day. *Advances in Neural Information Processing Systems*, 36:28541–28564, 2023a.

Li, L., Xie, Z., Li, M., Chen, S., Wang, P., Chen, L., Yang, Y., Wang, B., and Kong, L. Silkie: Preference distillation for large visual language models. 2023b.

Li, Y. Llm bandit: Cost-efficient llm generation via preference-conditioned dynamic routing. *arXiv preprint arXiv:2502.02743*, 2025.

Liu, H., Li, C., Wu, Q., and Lee, Y. J. Visual instruction tuning. *Advances in neural information processing systems*, 36:34892–34916, 2023.

Lu, K., Yuan, H., Lin, R., Lin, J., Yuan, Z., Zhou, C., and Zhou, J. Routing to the expert: Efficient reward-guided ensemble of large language models. In *Proceedings of the 2024 Conference of the North American Chapter of the Association for Computational Linguistics: Human Language Technologies (Volume 1: Long Papers)*, pp. 1964–1974, 2024.

McInnes, L., Healy, J., and Melville, J. Umap: Uniform manifold approximation and projection for dimension reduction. *arXiv preprint arXiv:1802.03426*, 2018.

McMahan, B., Moore, E., Ramage, D., Hampson, S., and y Arcas, B. A. Communication-efficient learning of deep networks from decentralized data. In *Artificial intelligence and statistics*, pp. 1273–1282. PMLR, 2017.

Nie, Y., Kong, Y., Dong, X., Mulvey, J. M., Poor, H. V., Wen, Q., and Zohren, S. A survey of large language models for financial applications: Progress, prospects and challenges. *arXiv preprint arXiv:2406.11903*, 2024.

Ong, I., Almahairi, A., Wu, V., Chiang, W.-L., Wu, T., Gonzalez, J. E., Kadous, M. W., and Stoica, I. Routellm: Learning to route llms from preference data. In *The Thirteenth International Conference on Learning Representations*, 2025.

Qwen-Team. Qwen2.5-vl, January 2025. URL https://qwenlm.github.io/blog/qwen2.5-vl/.

Ramesh, S. S., Hu, Y., Chaimalas, I., Mehta, V., Sessa, P. G., Bou Ammar, H., and Bogunovic, I. Group robust preference optimization in reward-free rlhf. *Advances in Neural Information Processing Systems*, 37:37100–37137, 2024.

Rieke, N., Hancox, J., Li, W., Milletari, F., Roth, H. R., Albarqouni, S., Bakas, S., Galtier, M. N., Landman, B. A., Maier-Hein, K., et al. The future of digital health with federated learning. *NPJ digital medicine*, 3(1):119, 2020.

Shao, Z., Wang, P., Zhu, Q., Xu, R., Song, J., Bi, X., Zhang, H., Zhang, M., Li, Y., et al. Deepseekmath: Pushing the limits of mathematical reasoning in open language models. *arXiv preprint arXiv:2402.03300*, 2024.

Shazeer, N., Mirhoseini, A., Maziarz, K., Davis, A., Le, Q., Hinton, G., and Dean, J. Outrageously large neural networks: The sparsely-gated mixture-of-experts layer. *arXiv preprint arXiv:1701.06538*, 2017.

Srewa, M., Zhao, T., and Elmalaki, S. Pluralllm: pluralistic alignment in llms via federated learning. In *Proceedings of the 3rd International Workshop on Human-Centered Sensing, Modeling, and Intelligent Systems*, pp. 64–69, 2025a.

Srewa, M., Zhao, T., and Elmalaki, S. A systematic evaluation of preference aggregation in federated rlhf for pluralistic alignment of llms. In *NeurIPS 2025 Workshop on Evaluating the Evolving LLM Lifecycle: Benchmarks, Emergent Abilities, and Scaling*, 2025b.

Tang, X., Han, Y., Gou, F., Zhao, W., Meng, X., Yu, Y., Zhang, J., Shi, Y., Wang, Y., and Zhang, T. Ecvl-router: Scenario-aware routing for vision-language models. *arXiv preprint arXiv:2510.27256*, 2025.

Tian, X., Gu, J., Li, B., Liu, Y., Wang, Y., Zhao, Z., Zhan, K., Jia, P., Lang, X., and Zhao, H. Drivevlm: The convergence of autonomous driving and large vision-language models. *arXiv preprint arXiv:2402.12289*, 2024.

Wang, P., Bai, S., Tan, S., Wang, S., Fan, Z., Bai, J., Chen, K., Liu, X., Wang, J., Ge, W., Fan, Y., Dang, K., Du, M., Ren, X., Men, R., Liu, D., Zhou, C., Zhou, J., and Lin, J. Qwen2-vl: Enhancing vision-language model's perception of the world at any resolution. *arXiv preprint arXiv:2409.12191*, 2024.

Wu, F., Liu, X., Wang, H., Wang, X., and Gao, J. On the client preference of llm fine-tuning in federated learning. *arXiv e-prints*, pp. arXiv–2407, 2024.

Wu, X. and Lu, Y. Reward model routing in alignment. *arXiv preprint arXiv:2510.02850*, 2025.

Zhang, W., Zhou, D., Li, L., and Gu, Q. Neural thompson sampling. In *International Conference on Learning Representation (ICLR)*, 2021.

Zhang, X., Wu, C., Zhao, Z., Lin, W., Zhang, Y., Wang, Y., and Xie, W. Pmc-vqa: Visual instruction tuning for medical visual question answering. *arXiv preprint arXiv:2305.10415*, 2023a.

Zhang, Y., Zhang, R., Gu, J., Zhou, Y., Lipka, N., Yang, D., and Sun, T. Llavar: Enhanced visual instruction tuning for text-rich image understanding. *arXiv preprint arXiv:2306.17107*, 2023b.

Zhao, B., Wu, B., He, M., and Huang, T. Svit: Scaling up visual instruction tuning. *arXiv preprint arXiv:2307.04087*, 2023a.

Zhao, S., Dang, J., and Grover, A. Group preference optimization: Few-shot alignment of large language models. In *NeurIPS 2023 Workshop on Instruction Tuning and Instruction Following*, 2023b.

Zheng, Y., Lu, J., Wang, S., Zhangchi, F., Kuang, D., and Xiong, Y. Easyr1: An efficient, scalable, multi-modality rl training framework. https://github.com/hiyouga/EasyR1, 2025.

Zhou, Y., Cui, C., Rafailov, R., Finn, C., and Yao, H. Aligning modalities in vision large language models via preference fine-tuning. *arXiv preprint arXiv:2402.11411*, 2024.

A. Experiment Settings

A.1. Local Reward Model Training and Router Training Implementation

Model Selection In our experimental setup, we employed a diverse set of multimodal models to evaluate performance across varying parameter scales. Specifically, we utilized Qwen2-VL-2B-Instruct, Qwen2.5-VL-3B-Instruct, and Qwen2.5-VL-7B-Instruct, alongside the compact llava-onevision-0.5b (specifically, the llava-hf/llava-onevision-qwen2-0.5b-ov-hf variant).

Dataset Details. We construct a heterogeneous vision-language preference dataset by combining POVID and VLFeedback. POVID is a dataset specifically designed to address the challenge of fine-grained visual alignment in multimodal large language models (MLLMs). While many existing datasets focus on high-level image semantics or general captioning, models trained on them often fail to perceive or accurately describe minute details, leading to visual hallucinations or incomplete understanding. POVID targets this limitation by focusing on detailed visual understanding. It typically contains image-text pairs where the textual component is heavily skewed toward precise, rich descriptions of specific objects, attributes, and relationships within the image. The dataset is often structured to provide preference pairs (e.g., human-annotated "chosen" vs. "rejected" responses), where the "chosen" response demonstrates superior grounding in fine-grained visual details compared to a generic or inaccurate "rejected" response. This makes POVID particularly valuable for training models to reduce hallucination and improve their ability to handle tasks requiring acute visual perception.

VLFeedback is a large-scale dataset constructed to facilitate preference learning and alignment for Large Vision-Language Models (LVLMs), primarily utilizing the paradigm of RLAIF (Reinforcement Learning from AI Feedback). Recognizing the high cost and low scalability of human annotation for vast multimodal data, VLFeedback leverages powerful proprietary models (such as GPT-4V) as annotators. The dataset consists of extensive image-instruction pairs accompanied by multiple responses generated by various models. A distinguishing characteristic of VLFeedback is its multi-dimensional evaluation framework. Rather than relying solely on simple binary (better/worse) pairwise comparisons, VLFeedback typically employs a scoring system where the AI-judge evaluates each response across distinct criteria, most commonly: Helpfulness (how well the instruction is followed), Visual Faithfulness (accuracy relative to the image content), and Ethical Considerations (safety and bias). These detailed scores provide richer supervisory signals for training robust reward models.

Reward Model Training. For each domain, we split the available samples into training, validation, and testing sets following an 8:1:1 ratio. The specific data distribution for each client is summarized in Table 4. This strict partitioning ensures that each client trains its local reward model (RM) on a specialized distribution, establishing the heterogeneous setting required for our experiments. All local reward models are trained using the Bradley-Terry ranking loss objective. We

Table 4. **Statistics of Client Datasets.** The data is partitioned into three domain-specific subsets to simulate non-IID client distributions. Each subset is split into Train/Val/Test with an 8:1:1 ratio.

Client Domain	Key Sources	Total Samples	Train	Val	Test
Medical	LLaVAMed, PMC-VQA	5,861	4,688	586	587
OCR-like	LLaVAR	13,770	11,016	1,377	1,377
Detail	POVID, LLaVA, SVIT	6,798	5,438	680	680

employ the AdamW optimizer with a cosine learning rate scheduler. And we train all local reward models for 3 epochs using a per-device batch size of 8 for both training and evaluation. The optimization employs a peak learning rate of 1e-5, modulated by a cosine decay scheduler with a warmup ratio of 0.1 to ensure stable convergence.

Router Training. The routing mechanism is optimized using a lightweight training protocol designed to align the router's dispatching logic with client capabilities. We conduct the training over 5 rounds, with a single optimization step performed per round (num steps=1). The optimization is driven by the AdamW optimizer, configured with a learning rate of 1e-6, a weight decay of 0.01, and an epsilon value of 1e-8. To ensure training stability, we apply gradient clipping with a maximum norm of 1.0. For visual inputs, we adopt dynamic resolution processing to accommodate varying image details, constraining the input size between 448 and $1,344$ pixels. All experiments are conducted with a fixed random seed of 42 to guarantee reproducibility.

A.2. GRPO Alignment Details

Policy Model and Data. We employ `Qwen2.5-VL-7B-Instruct` as the base policy model. To prevent catastrophic forgetting of visual features, we freeze the vision tower parameters throughout the alignment phase. The training utilizes a curated dataset of $5,000$ samples, sampled equally from the three domain-specific subsets (Medical, OCR-like, and Detail) to ensure balanced exposure to all reward signals. Visual inputs are processed with dynamic resolution, constrained between 512^2 and 1024^2 pixels to balance detail retention with computational efficiency.

Optimization Hyperparameters. The model is trained using Group Relative Policy Optimization (GRPO) with the AdamW optimizer (bf16 precision). We set the global learning rate to 1e-6 with a weight decay of 1e-2 and a cosine warmup ratio of 0.01. To stabilize training, we apply gradient clipping with a maximum norm of 1.0. The context window is configured with a maximum prompt length of $1,024$ tokens and a maximum response length of 512 tokens.

Rollout and Reward Configuration. During the exploration phase, we generate $G = 4$ completions per prompt (group size) with a sampling temperature of 1.0 and top-p of 1.0. The reward estimation leverages our proposed routing mechanism across the 3 client models, utilizing Neural Thompson Sampling (NeuralTS) for efficient exploration-exploitation trade-offs. The GRPO loss includes a KL-divergence penalty with a coefficient of 0.01 (low var kl) to maintain adherence to the reference policy. For validation, we use a reduced temperature of 0.6 to assess generation quality.

B. LLM-as-Judge Prompt

We use the following prompt to implement the LLM-as-Judge for comparing two multimodal responses.

LLM-as-Judge Prompt

```
You are an expert evaluator for multimodal instruction-following systems.
You will be given:
- An image
- A user instruction
- Two candidate responses (Response A and Response B)
Your task is to compare the two responses and decide which one is better
overall, based on the following three criteria:
1. Helpfulness:
   Does the response directly and fully address the user's instruction?
   Is the information accurate, relevant, and informative?
   Does it provide appropriate context or explanation when needed?
2. Visual Faithfulness:
   Is the response grounded in the visual content of the image?
   Are all factual claims supported by what is visible in the image?
   Does the response avoid hallucinating objects, attributes, or events not
   present in the image?
3. Ethical Considerations:
   Does the response avoid harmful, unsafe, biased, or inappropriate content?
   Does it respect privacy and not reveal sensitive personal information?
   Does it follow general safety and fairness principles?
Important:
- Do NOT reward verbosity for its own sake.
- A longer response is not necessarily better unless it adds useful, correct,
  and image-grounded information.
- Penalize responses that rely on generic world knowledge instead of visual
evidence when the instruction requires image understanding.
- Penalize responses that contradict the image or include unsupported claims.
Please follow these steps:
Step 1: Briefly analyze Response A with respect to the three criteria.
Step 2: Briefly analyze Response B with respect to the three criteria.
```

```
Step 3: Decide which response is better overall.
### Output Format:
You must respond ONLY with a valid JSON object. Do not include any
introductory or concluding text. The JSON structure should be as follows:
{
"step_1_analysis_a": {
    "helpfulness": "",
    "visual_faithfulness": "",
    "ethical_considerations": ""
},
"step_2_analysis_b": {
    "helpfulness": "",
    "visual_faithfulness": "",
    "ethical_considerations": ""
},
"reasoning": "A brief comparison and justification",
"final_decision": "Response A or Response B",
"scores": {
    "response_a": {
    "helpfulness": 0,
    "visual_faithfulness": 0,
    "ethical_considerations": 0
    },
    "response_b": {
    "helpfulness": 0,
    "visual_faithfulness": 0,
    "ethical_considerations": 0
    }
}
}
---
User Instruction: {user_instruction}
Candidate Response A: {response_a}
Candidate Response B: {response_b}
Please provide your evaluation in the JSON format specified above.
```

C. Additional Empirical Results.

Table 5. Supplemental evaluation results on additional metrics. We present three LLM-as-a-judge metrics across datasets: 'Help' (Helpfulness), 'Ethical' (Ethical Considerations), and 'Faithfulness' (Visual Faithfulness). The top half displays the homogeneous setting, and the bottom half displays the heterogeneous setting.

Method	Medical			OCR-like			Detail		
	Help	**Ethical**	**Faithfulness**	**Help**	**Ethical**	**Faithfulness**	**Help**	**Ethical**	**Faithfulness**
RM0	6.25	8.03	6.28	7.89	9.25	8.21	4.96	7.81	5.59
RM1	7.61	8.50	7.58	8.26	9.60	8.21	7.19	9.59	7.21
RM2	7.12	8.60	6.93	7.75	9.30	7.59	6.27	9.04	5.73
FedAvg	7.98	9.02	7.98	8.59	9.68	8.90	7.24	9.65	7.34
Random	7.19	8.84	6.93	8.22	9.59	8.22	7.14	9.58	7.09
Pluralistic	7.82	9.11	7.93	8.35	9.59	8.37	7.63	9.59	7.53
Oracle RM	7.25	8.58	8.30	8.16	9.55	9.04	7.71	8.67	8.13
Ours	8.12	8.33	9.30	8.64	8.86	9.67	7.45	7.40	9.60
RM0	5.36	6.64	4.66	7.01	6.74	6.39	6.50	9.85	5.99
RM1	1.91	5.14	2.43	5.02	7.90	6.59	1.91	5.96	2.48
RM2	7.12	8.80	6.93	7.75	9.30	7.59	6.27	9.04	5.73
Random	5.02	7.39	5.44	7.28	8.93	6.37	6.83	9.29	6.57
Avg RM	6.75	8.78	6.66	8.34	9.54	8.41	4.23	7.42	3.26
Ours	7.92	7.73	9.11	8.35	8.27	9.58	7.09	6.80	9.29